Desalination and Water Treatment
www.deswater.com

doi: 10.1080/19443994.2013.822336

52 (2014) 6342–6347
October

Taylor & Francis
Taylor & Francis Group

Erosion probability for biofilm modeling: analysis of trends

Chrysi S. Laspidou

Department of Civil Engineering, University of Thessaly, Pedion Areos, 38334 Volos, Greece
Email: laspidou@uth.gr

Received 17 April 2013; Accepted 19 June 2013

ABSTRACT

This study presents the strengths and weaknesses of a biofilm erosion probability algorithm that can be used in cellular automaton and individual-based biofilm simulation models. The erosion probability is calculated using data on localized biofilm mechanical properties, expressed through the composite biofilm Young's modulus—a measure of biofilm strength that varies in time and space—and on fluid hydrodynamic shear stress. Analysis of trends shows that biofilm detachment is the process that results from the competition between biofilm strength and hydrodynamic shear stress exerted on it by the fluid, with hydrodynamics being more important when biofilm strength is low and vice versa. From the modeling sample analyzed in this study, it is evident that for biofilms with cluster and mushroom formations, erosion probabilities are lower in the crevices formed between two clusters—where substrate is depleted—and higher at the top of the clusters where there is fresh biomass growth. When compared to other detachment methodologies extensively used by biofilm modeling researchers, such as the detachment speed that is a function of the square of the distance to the solid substratum, it is proved that the probability of erosion algorithm would give similar results.

Keywords: Biofilm modeling; Biofilm detachment; Biofilm erosion; Cellular automaton; UMCCA; Biofilm mechanical properties; Probability of detachment

1. Introduction

A biofilm consists of microorganisms attached to a solid surface, the substratum, having microbial cells embedded in a matrix of organic polymers (extracellular polymeric substances—EPS) produced by the cells [1]. Biofilms are ubiquitous in nature and are increasingly important in engineered processes for wastewater treatment [2]. Some biofilms are viewed as "good," and we try to promote their accumulation. Examples of good biofilms include those that are exploited in fixed-film processes used to treat contaminated water, wastewater and air, those that attach to stream beds and aquatic vegetation, leading to self-purification of water bodies, and those responsible for engineered or intrinsic bioremediation of contaminated groundwater [3]. Other biofilms are viewed as "bad," and we try to remove or prevent them. Bad biofilms include those that foul ship hulls and pipelines [4], thereby increasing friction loss and corrosion, those that cause "souring" of oil wells, and those that cause medical problems, such as infection related to implants. Furthermore, membrane processes used in water desalination are often affected by biofouling [5] caused by the development of biofilm on the membrane that can lead to its failure due to flux decline, membrane

biodegradation from bacterial by-products and increased salt passage due to biofilm-mediated salt accumulation.

Biofilms are highly diverse; they can be physically very thin, or thick, while the physical structure can be either dense and homogeneous, or heterogeneous with clusters and streamers of biomass intermingled with open channels [1]. One of the reasons for biofilm diversity is that many processes occur together as the biofilm forms, such as microbial growth and death, attachment and detachment [6]. Furthermore, they are characterized by strong gradients; thus, the processes occur in very different ways at the outer surface of the biofilm, compared with near the substratum. This article deals with biofilm detachment, which is the physical movement of microbial cells from the biofilm matrix. Detachment results in a loss of material from the biofilm, and these materials generally move to the liquid that is in contact with the biofilm. It can occur in three broad patterns: (1) erosion, a continuous process by which small pieces of biofilm are removed from the biofilm's outer surface; (2) sloughing, an abrupt loss of a large segment of the biofilm; and (3) scouring, or removal of large biofilm segments under the action of strong forces, such as abrasion or scraping [7]. Whether the goal is to encourage or discourage biofilm accumulation, detachment is one of the key determinants for how much biofilm accumulates, as well as its physical and microbiological characteristics. Biofilm detachment is an emerging research field. Clearly, biofilm mechanical properties such as biofilm strength and cohesion play an important role in defining detachment; physical hydrodynamic forces acting on the biofilm from the liquid surrounding it are also important factors [8].

Due to its complexity, biofilm simulation modeling is extensively used in order to predict biofilm formation and growth. Discrete particle biofilm models represent biomass in individual units and include two general model classes: cellular automata (CA) models, such as the Unified Multi-Component Cellular Automaton (UMCCA) model [6,9] and individual based models [10]. A comparison of the two types of models is presented in Laspidou et al. [11]. In UMCCA, the biofilm is treated as a composite material composed of four different phases, three solid biomass materials (active biomass (X_a), *EPS*, and residual inert biomass (X_{res})) and pores. Although critical for estimating detachment, experimental data on biofilm mechanical properties, such as tensile strength, cohesive strength, elastic modulus, shear modulus, viscoelastic strength, etc. are relatively scarce [12–14]. As shown in Aravas and Laspidou [15], there is great variability between reported measurements, usually attributed to measurement protocols and different biofilm environments during growth and biofilm characterization. Biofilm mechanical properties are mainly affected by density and porosity, quantities that vary from one biofilm to another and also through the biofilm thickness. Porosity decreases in biofilms that are subjected to compressive forces, since the pores collapse [16] and can be reduced to almost zero; conversely, porosity increases when biofilms are under tension. Changes in porosity bring about changes in the volume fractions of all phases throughout the biofilm column [17].

Biofilm detachment, as important as it may be, remains a poorly characterized phenomenon. Researchers that have conducted experiments may report detachment kinetics of limited value since they apply only to their specific system; others use arbitrary kinetics that are not descriptive enough and do not take into account biofilm mechanical properties. Hermanowicz [18] developed a simple function that includes both hydrodynamics and biofilm cohesion and expresses the probability of cell erosion. This probability is suitable for use in CA biofilm models. Laspidou et al. [19] advanced this concept by providing a methodology on how to quantify biofilm strength using localized concentrations of X_a, *EPS*, X_{res} and voids and on how to quantify local hydrodynamics and embody it in a CA model for biofilm growth. This article further advances this algorithm by analyzing trends in biofilm erosion probability modeling and comparing it with other modeling approaches used in integrated CA and individual-based modeling approaches included in multidimensional biofilm models.

2. Materials and methods

Laspidou et al. [19] presented a simple rule that can be incorporated in CA biofilm models, in order to deal with the lack of any detailed information on local biofilm detachment. For modeling compartments at the biomass/liquid interface—compartments with at least one empty neighbor—the probability of biofilm erosion (P) is defined as follows:

$$P = \frac{1}{1 + E_{comp/\tau_w}} \tag{1}$$

where E_{comp} is the composite biofilm Young's modulus (or elastic modulus), which is a measure of stiffness of an elastic material and is used herein as a measure of biofilm strength and potentially as a predictor of where biofilm is least likely to fail. E_{comp} is not uniform throughout the biofilm but varies in

time and space, as do the fractions of voids and solid biofilm components (active biomass X_a, *EPS* and residual dead biomass X_{res}); however, it is not a weighted average of the solid fractions, but it is calculated following a homogenization technique [16,17]. The hydrodynamic shear stress acting upon the biofilm (τ_w) is a function of fluid velocity, fluid density and friction factor f; a methodology on how to calculate τ_w is presented in Laspidou et al. [19]. Friction factor f is dimensionless and is a function of only Reynolds number for laminar flow; for turbulent flow, f is a function of Reynolds number and "relative roughness" ε/D, the dimensionless ratio of average biofilm size to the size of pipe or flow-cell in which biofilm grows.

To show how E_{comp} varies throughout the biofilm, Fig. 1 shows a modeling biofilm sample, which is an output of the CA model UMCCA [6] and it is 600 μm long and 280 μm deep. A solid substratum is assumed at the bottom of the sample, which develops in a "mushroom" shape, due to its growing conditions. The biofilm is plotted in shades of grey with dark pixels corresponding to high E_{comp} values and lighter pixels to smaller values. It is obvious that the bottom of the biofilm, which is over 200 days old, has the highest E_{comp} values (as high as 175 Pa) and only the top part of the mushroom has lower E_{comp} values. High composite density and Young's modulus values at the bottom of the biofilm—close to the substratum—are a result of almost zero voids for the old biofilm, which has had a lot of time to consolidate, very low-active biomass X_a and high X_{res} concentrations. The specifics on the conditions that lead to the formation of this biofilm are presented in Laspidou et al. [9,19].

The erosion probability is calculated only for the outer biofilm shell, that is, for the series of compartments that come in contact with the fluid. Fig. 2 shows the graph of erosion probabilities in a color graph for the outer biofilm shell, or only for the biofilm compartments that are in contact with the fluid. The next step is to examine how sensitive the biofilm erosion probability is to the hydrodynamic shear stress τ_w. Fig. 3 shows a graph of all erosion probability values shown in Fig. 2 as a function of τ_w; in Fig. 2, the value of $\tau_w = 10$ Pa was used for the calculation of P, while in Fig. 3 probabilities are recalculated for τ_w equal to 5 and 20 Pa.

The last step of this analysis is to compare the probability of erosion calculation to other detachment algorithms that have been used extensively by other researchers. Xavier et al. [20] model detachment by erosion using a speed of detachment (F_{det}) that is a function of the square of the distance to the solid substratum (x), or $F_{det}(x) = k_{det}x^2$, where k_{det} is the detachment speed coefficient, with dimensions $L^{-1}T^{-1}$. A second-order dependence on the distance to the solid substrate was chosen by Xavier et al. [20], because it ensures the existence of a steady state, even for the extreme case of unlimited growth for the entire biofilm. They used several detachment speed coefficients, ranging from 0.95 to 95 $m^{-1}h^{-1}$. In this study, the detachment speed F_{det} is calculated for the UMCCA biofilm sample shown in Fig. 1 and it is compared with the probability of erosion P (Fig. 4), using a k_{det} value of 1/m-h. Obviously, it is possible to calculate only one value of F_{det} for every value of x, although there may exist multiple values of P for the same distance from the substratum x. For example, most of the

Fig. 1. Map of E_{comp} throughout the biofilm for an UMCCA sample. Values in the legend are in Pa. The conditions relevant to the development of this sample appear in Laspidou and Rittmann [9]. Figure is adapted from Laspidou et al. [19].

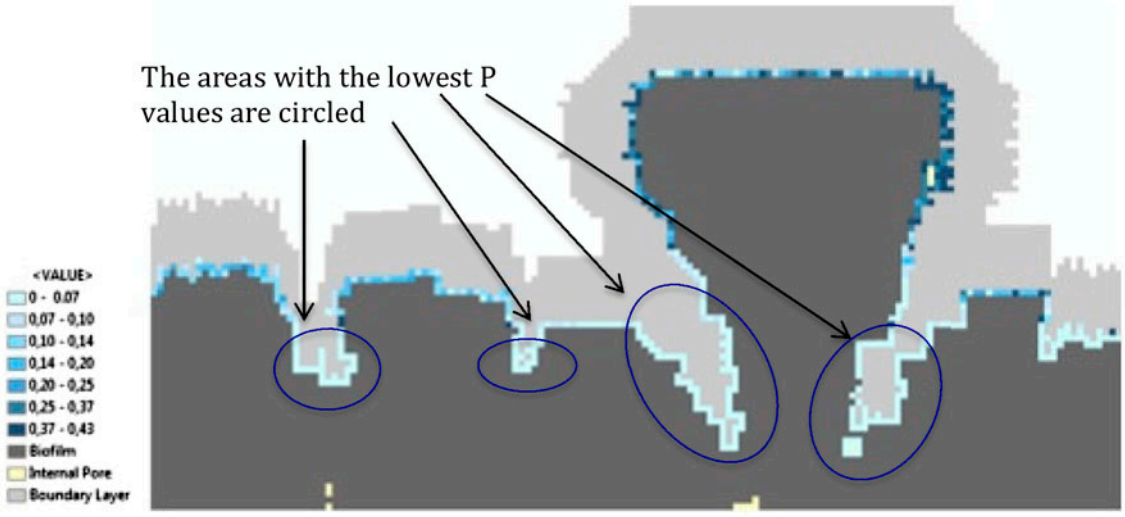

Fig. 2. Map of probability of detachment P for the outer shell of the UMCCA biofilm sample shown in Fig. 1: Probability is reported only for biofilm compartments that are in contact with fluid (adapted from Laspidou et al. [19]). For this calculation, it is assumed that $\tau_w = 10\,\text{Pa}$.

"mushroom" top has CA compartments that are at the same distance from the substratum; however, the erosion probability values vary, as shown in Fig. 2. In order to better compare the two quantities (F_{det} and P), an average P value is calculated for all x's; in other words, in Fig. 4, the P values plotted and compared with F_{det} are average values of all erosion probabilities corresponding to the same distance from the substratum x.

3. Results and discussion

In Fig. 2, the probability of erosion at the outer shell of the biofilm is plotted and the results appear to have a physical meaning. In Fig. 2, the parts of the biofilm that exhibit the smallest erosion probabilities are circled. It is obvious that these parts of the biofilm are somewhat protected by the flow, since they lie on a "fold" of the biofilm formation, or "crevice." According to the algorithm, these biofilm parts appear to have the lowest P values and will be the least likely to erode. This is a fortuitous result, since the erosion probability calculation does not explicitly include the flow field to make possible such a distinction between parts of the biofilm that are protected by the flow and parts that are more exposed to it. The reason why these areas have consistently shown a lower erosion probability is related to

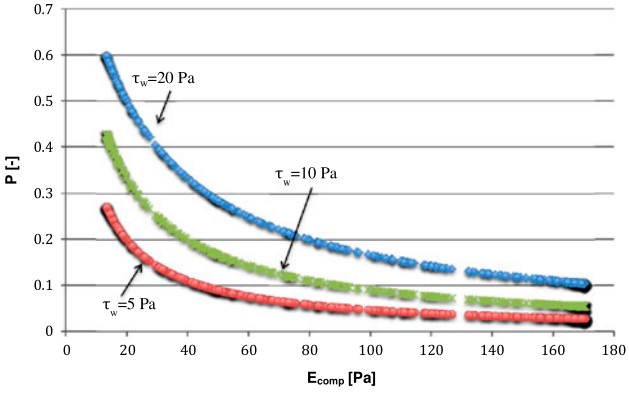

Fig. 3. Dimensionless erosion probabilities P for the biofilm modeling sample shown in Fig. 2, with variable localized E_{comp}, as shown in Fig. 1 and three different values of hydrodynamic shear stress τ_w.

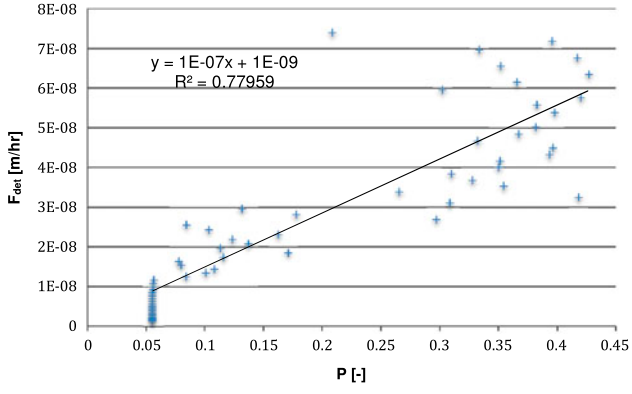

Fig. 4. Relationship between speed of detachment $F_{det}(x) = k_{det}x^2$ as reported in Xavier et al. [20] and erosion probability P for the biofilm modeling sample shown in Fig. 1. k_{det} is the detachment speed coefficient and x is the distance to the solid substratum. For this calculation, $k_{det} = 1\,\text{m}^{-1}\text{h}^{-1}$.

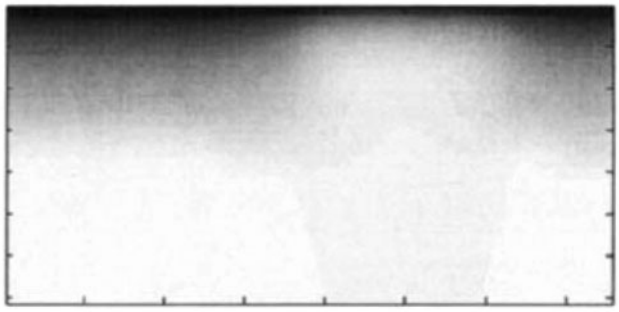

Fig. 5. Variability of substrate concentration in the fluid surrounding the biofilm sample. Darker and lighter pixels indicate higher and lower substrate concentrations, respectively. Adapted from Laspidou and Rittmann [9].

the composite Young's modulus E_{comp} of the biofilm. The lower P areas happen to have biofilm with the highest strength, that is, the highest localized E_{comp}; this is the case because those areas have very little new biofilm growth, as the substrate in those areas is depleted. Fig. 5 shows a shading plot of the substrate concentration of the fluid in which biofilm grows. In a sense, concentrations follow the shape of biofilm clusters, with lighter areas inside the clusters—due to depletion of substrate—and darker areas where there is biomass growth. The clusters that protrude highest have a higher substrate concentration at their outer surface and this gives them a growth advantage that leads to "mushroom" formations with new growth, which in turn, leads to lower E_{comp} values and higher erosion probabilities. Biomass in the biofilm "crevices" see almost zero concentration and cannot grow, but accumulate inert biomass, consolidate with time, have a porosity of almost zero and exhibit high E_{comp} values, which translate to low erosion probabilities.

Fig. 3 shows the dependence of erosion probability on hydrodynamic shear stress. As expected, higher τ_w values result in higher erosion probabilities. The figure shows that this dependence is stronger for lower biofilm Young's modulus values; this dependence gets weaker as E_{comp} values increase. This conclusion enhances the idea that biofilm detachment is the process that balances the competition between biofilm cohesiveness and strength and hydrodynamic shear stress. Only a small hydrodynamic stress is enough to cause biofilm erosion in a low-strength biofilm (low E_{comp}), while even high hydrodynamic stresses may be unlikely to cause erosion in a high-strength biofilm (high E_{comp}).

Fig. 4 shows the relationship of erosion probability to detachment speed used in several CA and individual-based modeling approaches [20]. Although the two quantities (F_{det} and P) are not directly comparable, since they have different units, a comparison of their trends is valuable. Plotting one quantity against the other is a way to see how they relate. The fact that erosion probability increases with detachment speed proves that there is a good agreement between the two quantities. The coefficient of determination R^2 for this specific sample is also relatively high (0.78) indicating that when either one of the two erosion prediction algorithms is used, biofilm erosion results will be generally similar, offering another indication that the erosion probability presented in this article is appropriate to predict biofilm erosion.

4. Conclusions

An analysis of the validity and robustness of an algorithm to calculate probability of biofilm erosion—a form of biofilm detachment—appropriate for use in CA models is presented in this article. The trends that influence the probability of erosion are described and analyzed. It is shown that the proposed erosion probability calculation gives results that have a physical meaning that is consistent with biofilm growing conditions, showing higher erosion in areas exposed to high fluid hydrodynamic stresses and lower erosion overall in parts of the biofilm that clusters "fold" or form crevices, that are expected to be protected from the flow, but also have low substrate concentration. Erosion probabilities are computed using the localized composite biofilm Young's modulus (E_{comp}) and the hydrodynamic shear stress τ_w. Analysis of results proves that biofilm detachment is the process that results from the competition between biofilm cohesiveness and strength and hydrodynamic shear stress. When compared with other detachment methodologies used by researchers for CA and individual-based models, such as the detachment speed F_{det}, it is proved that the probability of erosion algorithm would give similar results.

References

[1] B.E. Rittmann, P.L. McCarty, Environmental Biotechnology: Principles and Applications, McGraw-Hill, New York, NY, 2000.
[2] T. Yu, W. Lin, B.S. McSwain, M. Yu, X. Zhang, Biological fixed film systems—Review, Water Environ. Res. 78 (2006) 1324–1362.
[3] B.E. Rittmann, *In Situ* Bioremediation, 2nd ed., Noyes Publ, Park Ridge, IL, 1994.
[4] L.M. Zhai, J. Yin, C. Wang, J.-C. Huang, Biofilm sloughing and CBP formation in a 12-km transport system carrying chlorinated saline secondary effluent, Desalin. Water Treat. 19 (2010) 57–63.
[5] E. Bar-Zeev, I. Berman-Frank, B. Liberman, E. Rahav, U. Passow, T. Berman, Transparent exopolymer particles: Potential agents for organic fouling and biofilm formation in desalination and water treatment plants, Desalin. Water Treat. 3 (2009) 136–142.

[6] C.S. Laspidou, B.E. Rittmann, Modeling the development of biofilm density including active bacteria, inert biomass and extracellular polymeric substances, Water Res. 38 (2004) 3349–3361.
[7] B.E. Rittmann, C.S. Laspidou, Biofilm detachment, in: G. Bitton (Ed.), Encyclopedia of Environmental Microbiology, John Wiley & Sons, New York, NY, 2002, pp. 544–550.
[8] P. Ramasamy, X. Zhang, Effects of shear stress on the secretion of extracellular polymeric substances in biofilm, Water Sci. Technol. 52 (2005) 217–223.
[9] C.S. Laspidou, B.E. Rittmann, Evaluating trends in biofilm density using the UMCCA model, Water Res. 38 (2004) 3362–3372.
[10] J.B. Xavier, C. Picioreanu, M.C.M. Van Loosdrecht, A framework for multidimensional modeling of activity and structure of multispecies biofilms, Environ. Microbiol. 7 (2005) 1085–1103.
[11] C.S. Laspidou, A. Kungolos, P. Samaras, Cellular-Automata and individual-based approaches for the modeling of biofilm structures: Pros and cons, Desalination 250 (2009) 390–394.
[12] P. Stoodley, Z. Lewandowski, J.D. Boyle, H.M. Lappin-Scott, Structural deformation of bacterial biofilms caused by short-term fluctuations in fluid shear: An *in situ* investigation of biofilm rheology, Biotechnol. Bioeng. 65 (1999) 83–92.
[13] E.H. Poppele, R. Hozalski, Micro-cantilever method for measuring the tensile strength of biofilms and microbial flocs, J. Microbiol. Methods 55 (2003) 607–615.
[14] V. Körstgens, H.-C. Flemming, J. Wingender, W. Borchard, Uniaxial compression measurement device for investigation of the mechanical stability of biofilms, J. Microbiol. Methods 46 (2001) 9–17.
[15] N. Aravas, C. Laspidou, On the calculation of the elastic modulus of a biofilm streamer, Biotechnol. Bioeng. 101 (2008) 196–200.
[16] C.S. Laspidou, N. Aravas, Variation in the mechanical properties of a porous multi-phase biofilm under compression due to void closure, Water Sci. Technol. 55 (2007) 447–453.
[17] C.S. Laspidou, B.E. Rittmann, S.A. Karamanos, Finite element modeling to expand the UMCCA model to describe biofilm mechanical behavior, Water Sci. Technol. 52 (2005) 161–166.
[18] S.W. Hermanowicz, A simple 2D biofilm model yields a variety of morphological features, Math. Biosci. 169 (2001) 1–14.
[19] C.S. Laspidou, A. Liakopoulos, M.G. Spiliotopoulos, A 2D cellular automaton biofilm detachment algorithm, Lecture Notes in Comput. Sci. 7495 (2012) 415–424.
[20] J.B. Xavier, C. Picioreanu, M.C.M. van Loosdrecht, A general description of detachment for multidimensional modelling of biofilms, Biotechnol. Bioeng. 91 (2005) 651–669.